PHYSICAL REVIEW C **78**, 017302 (2008)

Intermediate-energy Coulomb excitation of ^{30}Na

S. Ettenauer,[1,*] H. Zwahlen,[1,2] P. Adrich,[1] D. Bazin,[1] C. M. Campbell,[1] J. M. Cook,[1,2] A. D. Davies,[1,2] D.-C. Dinca,[1,2] A. Gade,[1,2] T. Glasmacher,[1,2] J.-L. Lecouey,[1] W. F. Mueller,[1] T. Otsuka,[3,4] R. R. Reynolds,[5] L. A. Riley,[6] J. R. Terry,[1,2] Y. Utsuno,[7] and K. Yoneda[1]

[1]*National Superconducting Cyclotron Laboratory, Michigan State University, East Lansing, Michigan 48824, USA*
[2]*Department of Physics and Astronomy, Michigan State University, East Lansing, Michigan 48824, USA*
[3]*Department of Physics and Center for Nuclear Study, University of Tokyo, Hongo, Tokyo 113-0033, Japan*
[4]*RIKEN, Hirosawa, Wako-shi, Saitama 351-0198, Japan*
[5]*Department of Physics, Florida State University, Tallahassee, Florida 32306, USA*
[6]*Department of Physics and Astronomy, Ursinus College, Collegeville, Pennsylvania 19426, USA*
[7]*Japan Atomic Energy Research Institute, Tokai, Ibaraki 319-1195, Japan*

(Received 2 April 2008; published 15 July 2008)

The neutron-rich nucleus ^{30}Na in the vicinity of the "Island of Inversion" was investigated using intermediate-energy Coulomb excitation. A single γ-ray transition was observed and attributed to the $3_1^+ \rightarrow 2_{gs}^+$ decay. A transition probability of $B(E2; 2_{gs}^+ \rightarrow 3_1^+) = 147(21)\, e^2\,\mathrm{fm}^4$ was determined and found in agreement with a previous experiment and with large-scale shell-model calculations. Evidence for the strong excitation of the 4_1^+ state predicted by the shell-model calculations was not observed.

DOI: 10.1103/PhysRevC.78.017302 PACS number(s): 25.70.De, 27.30.+t

The properties of neutron-rich nuclei in the vicinity of ^{31}Na are characterized by the presence of neutron "intruder" configurations near the ground states. These are $(sd)^{-n}(pf)^{+n}$ particle-hole excitations across the $N = 20$ shell gap [1], which is significantly narrowed in this region. The attractive $T = 0$ monopole interaction between the $\pi d_{5/2}$ and $\nu d_{3/2}$ orbits changes the size of the $N = 20$ effective energy gap as protons fill the $d_{5/2}$ orbit [2] and leads to the formation of the so-called "Island of Inversion" where intruder configurations are energetically favored over the normal configurations. Originally, the "Island of Inversion" was proposed to contain neon, sodium, and magnesium isotopes with $N = 20$–22 [1]. Recent experiments expanded the Island of Inversion and probed the transitional regions in magnesium [3–5], sodium [6–9], and neon isotopes [10,11].

Large-scale Monte-Carlo Shell-Model (MCSM) calculations with the SDPF-M effective interaction [12] allow for the unrestricted mixing of normal and intruder configurations and provide a consistent description of their competition in the transitional regions. The properties of the sodium isotopes $^{27-31}$Na have been calculated in this approach in detail and ^{30}Na has been identified as the key nucleus because its 2p2h intruder probability in the ground state depends more sensitively on the size of the effective sd-fp shell gap than for any other sodium isotope [13]. Nuclear structure information on this nucleus thus poses rigorous tests for calculations in this region. A recent β-decay measurement demonstrated that a number of intruder dominated states lie below levels dominated by normal configurations in ^{30}Na [9].

The MCSM calculations predict ^{30}Na to be a well-deformed, prolate rotor with a $K = 2$ band built on the 2^+ ground state. The 3_1^+ and 4_1^+ of this band structure are expected to have strong $E2$ transition matrix elements to the ground state [13]. Inelastic proton scattering performed at RIKEN [14] and intermediate-energy Coulomb excitation performed at the National Superconducting Cyclotron Laboratory (NSCL) [6] showed that ^{30}Na is strongly deformed with the proton and neutron deformations in phase. Both inelastic scattering experiments reported a γ-ray transition at 433(16) and 403(18) keV, respectively, attributed to the decay of the 3_1^+ excited state to the 2^+ ground state. From the NSCL Coulomb-excitation experiment, a $B(E2; 2_{gs}^+ \rightarrow 3_1^+) = 130^{+90}_{-65} e^2\,\mathrm{fm}^4$ value was deduced, confirming the large degree of collectivity and in agreement with $B(E2; 2_{gs}^+ \rightarrow 3_1^+) = 168 e^2\,\mathrm{fm}^4$ from the MCSM. However, this value for the excitation strength was obtained by subtracting an estimated feeding contribution from the *unobserved* 4^+ state of the $K = 2$ band. A second γ-ray transition was observed in the spectrum at 701(20) keV but was attributed to ^{29}Na produced in the one-neutron removal channel, which could not be discriminated at that time [6].

In the present article we report on the intermediate-energy Coulomb excitation of ^{30}Na $+^{209}$ Bi at 80.1 MeV/nucleon midtarget energy with the highly segmented germanium array SeGA for γ-ray detection and the large-acceptance S800 magnetic spectrograph for particle identification and scattering-angle reconstruction. The prior Coulomb excitation measurement, ^{30}Na $+^{197}$Au at 55.6 MeV/nucleon by Prity-chenko *et al.* [6] used a NaI(Tl) array with moderate energy resolution for the γ-ray detection and a phoswich detector with a fixed opening angle for particle identification and the determination of the maximum scattering angle.

The Coupled-Cyclotron Facility of the NSCL at Michigan State University provided a primary beam of ^{48}Ca with 140 MeV/nucleon impinging upon a ^{9}Be fragmentation target of 1151 mg/cm^2 thickness located at the midacceptance target position of the A1900 fragment separator [15]. A 450 mg/cm^2 aluminum wedge degrader was used to select the

*Present address: TRIUMF, 4004 Wesbrook Mall, Vancouver, B.C. V6T 2A3, Canada.

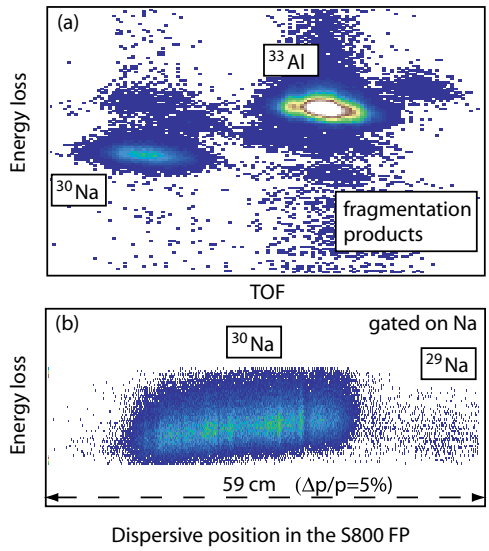

FIG. 1. (Color online) (a) Energy loss vs TOF for the reacted projectiles emerging from the ^{209}Bi target. ^{30}Na can be cleanly identified from the other constituents of the cocktail beam. (b) Energy loss vs dispersive position in the S800 focal plane gated on the ^{30}Na projectiles identified via (a). Shown is the entire acceptance of the spectrograph in the dispersive direction. A tail of the ^{29}Na distribution originating from the (weak) one-neutron knockout channel enters the spectrograph at the edge of the acceptance. ^{30}Na can be cleanly separated.

secondary beam. The total momentum acceptance was restricted to 2%.

The Coulomb excitation target, 737.2 mg/cm^2 thick ^{209}Bi, was located at the target position of the S800 spectrograph [16]. The ionization chamber and the position-sensitive cathode readout drift chambers of the S800 focal-plane detector system and plastic timing detectors served to unambiguously identify the reacted projectiles emerging from the target. In conjunction with the beam optics and the known magnet settings of the spectrograph, the scattering angles of the reacted ^{30}Na projectiles were reconstructed event-by-event.

The particle identification spectra are shown in Fig. 1. Plotted is the energy loss measured with the ionization chamber vs the time of flight (TOF) measured between two plastic scintillators [Fig. 1(a)] and the energy loss vs the dispersive position in the S800 focal plane [Fig. 1(b)]. The constituents of the neutron-rich cocktail beam—the main components ^{33}Al and ^{30}Na and minor constituents ^{32,31}Mg and ^{35}Si—can be clearly identified. Compared to the cross section for (in)elastic scattering, the one-neutron removal from ^{30}Na to ^{29}Na proceeds at a low rate. The spectrum in Fig. 1(b) is gated on the ^{30}Na identified from the spectrum shown in Fig. 1(a). The momentum of the one-nucleon knockout residues ^{29}Na is about 3.3% lower than the momentum of ^{30}Na passing through the target. The ^{30}Na projectiles can be clearly identified from their position in the focal plane and, as apparent from the spectrum, only the tail of the ^{29}Na distribution enters the focal plane at the edge of the acceptance.

The reaction target was surrounded by NSCL's segmented germanium detector array SeGA [17]. Each detector is 32-fold segmented; the high degree of segmentation is needed to Doppler reconstruct the γ rays emitted by the reacted nuclei in fight. The 18 detectors of SeGA were arranged in nine angle pairs at 24°, 29°, 40°, 60°, 78°, 90°, 126°, 139°, and 147° with respect to the beam axis. GEANT simulations were employed to simulate the response of the array and to correct the γ-ray efficiency of the setup measured with stationary sources for the Lorentz boost arising from the emission in flight. A relative uncertainty of 5% is assumed for the in-beam γ-ray detection efficiency.

While beam energies below the Coulomb barrier prevent nuclear contributions to the excitation process, very peripheral collisions must be chosen in the regime of intermediate-energy Coulomb excitation to ensure the dominance of the electromagnetic interaction. This can be realized by restricting the analysis to scattering events at extremely forward angles, corresponding to large impact parameters, $b_{\min}$, in the collisions of projectile and target nuclei [18]. The distance $1.2A_p^{1/3} + 1.2A_t^{1/3} + 2$ fm $= 12.9$ fm ("touching sphere + 2 fm") was considered sufficient to ensure the dominance of the electromagnetic excitation, justified in comparison to coupled-channels calculations as discussed later. The midtarget energy of the ^{30}Na beam was 80.1 MeV/nucleon, resulting in a minimum impact parameter of $b_{\min} = 12.9$ fm for a maximum scattering angle of $\theta_{\rm lab}^{\max} = 2.52°$. A software gate on the scattering-angle spectrum reconstructed with the S800 spectrograph was used to restrict the analysis to events with impact parameters exceeding 12.85 fm.

Figure 2 displays event-by-event Doppler reconstructed γ-ray spectra recorded in coincidence with scattered ^{30}Na nuclei (a) for events restricted to the maximum scattering

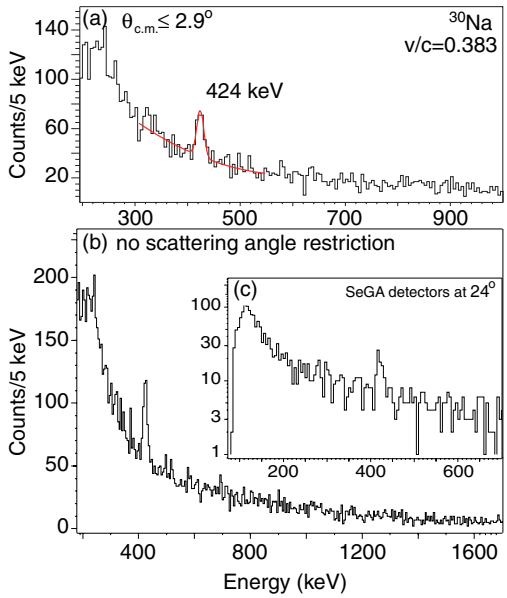

FIG. 2. (Color online) (a) γ-ray spectrum in coincidence with scattered ^{30}Na (maximum scattering angle $\theta_{\rm c.m.}^{\max} = 2.90°$). The γ rays detected in the laboratory were event-by-event Doppler reconstructed into the rest frame of the projectile. (b) Same as (a) but without a software gate applied that restricts events to $\theta \leqslant \theta^{\max}$. (c) Same as (b) only for the SeGA detector pair at 24° with respect to the beam axis.

angle of $\theta_{\rm lab}^{\rm max} = 2.52^\circ$ (corresponds to $\theta_{\rm c.m.}^{\rm max} = 2.90^\circ$), (b) without any restriction on the scattering angle, and (c) for the SeGA detector pair at the most forward angle with respect to the beam axis. Only one photopeak, $E_\gamma = 424(3)$ keV, was observed in coincidence with ^{30}Na. Due to the Lorentz boost, the most forward detectors can detect the lowest-energy γ rays; in our experiment, γ-ray detection was possible above 125 keV [see Fig. 2(c)]. The γ-ray energy is in agreement with the previous inelastic scattering experiments [6,14]. We note that the additional γ ray reported at 701 keV from the previous Coulomb excitation experiment by Pritychenko *et al.* [6] is not observed here because the ^{29}Na produced in the one-neutron knockout reaction could be discriminated by the particle-identification capabilities of the S800 spectrograph (see Fig. 1).

An angle-integrated Coulomb excitation cross section of $\sigma(\theta \leqslant 2.9^\circ_{\rm c.m.}) = 41(5)$ mb was derived for the excitation of the 424 keV state from the efficiency-corrected γ-ray intensity obtained from the spectrum shown in Fig. 2(a) relative to the number of scattered projectiles per number density of the target.

Measured cross sections can be translated into absolute $B(E2\uparrow)$ excitation strengths in a robust and precise way—as shown by extensive studies and comparisons [19–22]—using the Winther–Alder theory of relativistic Coulomb excitation [23]. In agreement with previous experiment, we attribute the 424 keV γ ray to the decay of the 3_1^+ state to the 2^+ ground state. Assuming pure $E2$ character to the transition, our experimental cross section yields $B(E2; 2_{\rm gs}^+ \rightarrow 3_1^+) = 150(21)\, e^2\,{\rm fm}^4$, consistent with the result by Pritychenko *et al.* [6] and in agreement with the prediction by the MCSM of $B(E2; 2_{\rm gs}^+ \rightarrow 3_1^+) = 168\, e^2\,{\rm fm}^4$ [13]. A systematic uncertainty of 6.7% is attributed to a 0.1° uncertainty in the scattering-angle reconstruction and has been added in quadrature to the statistical uncertainty. However, it was not possible to determine the multipolarity of the γ-ray transition and $M1$ character cannot a priori be excluded. The MCSM predicts a rather large magnetic excitation strength with $B(M1; 2_{\rm gs}^+ \rightarrow 3_1^+) = 0.268\mu_N^2$. This $B(M1)$ value corresponds to an angle-integrated cross section of $\sigma = 0.9$ mb and a corrected excitation strength of $B(E2; 2_{\rm gs}^+ \rightarrow 3_1^+) = 147(21)\, e^2\,{\rm fm}^4$ that takes into account an $M1$ strength calculated within the shell model.

Pritychenko *et al.* [6] extracted the $B(E2)$ value from coupled-channels calculations that took into account the nuclear contribution to the excitation process. Here, we assumed pure Coulomb excitation and we used coupled-channels calculations to estimate the nuclear contribution. The interaction of ^{30}Na+^{209}Bi at 80 MeV/nucleon was calculated with the ECIS95 coupled-channels code [24]. The angular distribution for the $2_{\rm gs}^+ \rightarrow 3_1^+$ excitation cross section was calculated (i) with the Coulomb interaction only and (ii) with Coulomb and nuclear interactions enabled. Two optical potential parameter sets were used, ^{16}O+^{208}Pb at 50 MeV/nucleon [25] and ^{17}O+^{208}Pb at 84 MeV/nucleon [26]. From the difference between the angle-integrated excitation cross sections with and without nuclear interactions enabled we find that the nuclear contribution within our scattering-angle range is 2% for the optical potential of Ref. [25] and 0.4% for the optical potential

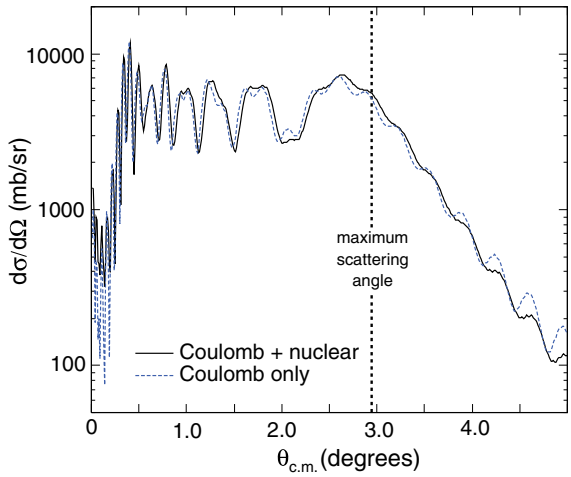

FIG. 3. (Color online) ECIS95 calculations for ^{30}Na +^{209}Bi at 80 MeV/nucleon. Given are differential cross sections for the $2_{\rm gs}^+ \rightarrow 3_1^+$ excitation as a function of the center-of-mass angle for solely Coulomb excitation (blue, dashed line) and for Coulomb excitation plus nuclear contribution (black, solid line). The optical potential from Ref. [25] was used for this plot.

of Ref. [26]. Figure 3 shows the angular distributions for the example of the optical potential parameter set of Ref. [25]. The very small nuclear contributions validate our analysis based on the Winther–Alder formalism also for this case with $Z_p = 11$.

The MCSM calculations based on the SDPF-M effective interaction predict $B(E2; 2_{\rm gs}^+ \rightarrow 3_1^+) = 168\, e^2\,{\rm fm}^4$ at 430 keV and $B(E2; 2_{\rm gs}^+ \rightarrow 4_1^+) = 90\, e^2\,{\rm fm}^4$ at 800 keV to constitute the low-lying $E2$ strength in ^{30}Na. In all scattering experiments, only one γ-ray transition was detected and identified with the $3_1^+ \rightarrow 2_{\rm gs}^+$ transition. The corresponding excitation strength $B(E2; 2_{\rm gs}^+ \rightarrow 3_1^+) = 147(21)\, e^2\,{\rm fm}^4$ deduced in the present work is in agreement with the MCSM prediction at significantly reduced uncertainty compared to the previous result of $B(E2; 2_{\rm gs}^+ \rightarrow 3_1^+) = 130^{+90}_{-65}\, e^2\,{\rm fm}^4$. Figure 4 summarizes the theoretical and experimental $E2$ strength distribution for excitations from the ground state of ^{30}Na. A $B(E2; 2_{\rm gs}^+ \rightarrow 4_1^+) = 90\, e^2\,{\rm fm}^4$ excitation strength at 800 keV, assuming that

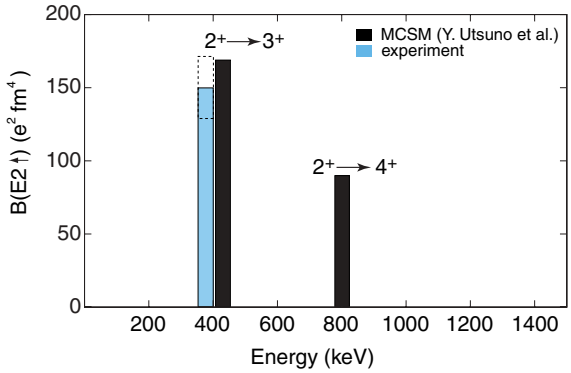

FIG. 4. (Color online) Calculated $B(E2; 2_{\rm gs}^+ \rightarrow J^+)$ strengths within the MCSM using the SDPF-M effective interaction compared to the experimental result.

the only branch is the decay to the ground state, would correspond to a cross section of $\sigma = 25$ mb or, with an in-beam γ-ray efficiency of 3.0% at 800 keV, 55 counts in a photopeak in Fig. 2(a). In the MCSM, the 4_1^+ state of the $K = 2$ band is predicted to exhibit a strong intraband decay to the 3_1^+ state with a transition strength of $B(M1; 4_1^+ \rightarrow 3_1^+) = 0.43\mu_N^2$. In this scenario, there would be a photopeak with more than 70 counts at about 370 keV corresponding to the $4_1^+ \rightarrow 3_1^+$ transition. Also, more than 50% of the population of the 3_1^+ state would have to be attributed to feeding by the 4_1^+ state, leading to a small $B(E2; 2_{gs}^+ \rightarrow 3_1^+)$ value extracted from experiment. To reduce this $B(E2)$ value (due to feeding) beyond the experimental uncertainty, a photopeak with 18 counts would have to be present at about 370 keV. As can be seen in Fig. 2, there is no evidence for a photopeak at 370 or 800 keV.

In summary, we have performed intermediate-energy Coulomb excitation of ^{30}Na projectiles impinging upon a ^{209}Bi target. A single γ-ray transition was observed and attributed to the $3_1^+ \rightarrow 2_{gs}^+$ decay in agreement with previous experiments. The corresponding $B(E2; 2_{gs}^+ \rightarrow 3_1^+) = 147(21)\, e^2\,\mathrm{fm}^4$ excitation strength deduced from the measured Coulomb excitation cross section agrees with large-scale MCSM calculations using the SDPF-M effective interaction. However, within the MCSM, the 3_1^+ state is thought to be member of a $K = 2$ rotational band and evidence for the predicted 4^+ state of this band structure, with a significant transition matrix element to the 2^+ ground state and a strong intraband decay to the 3^+ state, can be excluded from the present data. The new results provide an important indication that the shell-model description in the vicinity of the Island of Inversion must be improved to describe the details of odd-odd nuclei.

This work was supported by the National Science Foundation under Grants PHY-0606007 and PHY-0653323 and in part by a Grant-in-Aid for Specially Promoted Research (No. 13002001) from the MEXT.

[1] E. K. Warburton, J. A. Becker, and B. A. Brown, Phys. Rev. C **41**, 1147 (1990).
[2] T. Otsuka, R. Fujimoto, Y. Utsuno, B. A. Brown, M. Honma, and T. Mizusaki, Phys. Rev. Lett. **87**, 082502 (2001).
[3] G. Neyens *et al.*, Phys. Rev. Lett. **94**, 022501 (2005).
[4] J. R. Terry *et al.*, Phys. Rev. C **77**, 014316 (2008).
[5] A. Gade *et al.*, Phys. Rev. Lett. **99**, 072502 (2007).
[6] B. V. Pritychenko *et al.*, Phys. Rev. C **65**, 061304(R) (2002).
[7] V. Tripathi *et al.*, Phys. Rev. Lett. **94**, 162501 (2005).
[8] V. Tripathi *et al.*, Phys. Rev. C **73**, 054303 (2006).
[9] V. Tripathi *et al.*, Phys. Rev. C **76**, 021301(R) (2007).
[10] J. R. Terry *et al.*, Phys. Lett. **B640**, 86 (2006).
[11] A. Obertelli *et al.*, Phys. Lett. **B633**, 33 (2006).
[12] Y. Utsuno, T. Otsuka, T. Mizusaki, and M. Honma, Phys. Rev. C **60**, 054315 (1999).
[13] Y. Utsuno, T. Otsuka, T. Glasmacher, T. Mizusaki, and M. Honma, Phys. Rev. C **70**, 044307 (2004).
[14] Z. Elekes *et al.*, Phys. Rev. C **73**, 044314 (2006).
[15] D. J. Morrissey *et al.*, Nucl. Instrum. Methods Phys. Res. B **204**, 90 (2003).
[16] D. Bazin *et al.*, Nucl. Instrum. Methods Phys. Res. B **204**, 629 (2003).
[17] W. F. Mueller *et al.*, Nucl. Instrum. Methods A **466**, 492 (2001).
[18] T. Glasmacher, Annu. Rev. Nucl. Part. Sci. **48**, 1 (1998).
[19] A. Gade *et al.*, Phys. Rev. C **68**, 014302 (2003).
[20] J. M. Cook, T. Glasmacher, and A. Gade, Phys. Rev. C **73**, 024315 (2006).
[21] F. Delaunay and F. Nunes, J. Phys. G **34**, 2207 (2007).
[22] H. Scheit *et al.*, Phys. Lett. **B659**, 515 (2008).
[23] A. Winther and K. Alder, Nucl. Phys. **A319**, 518 (1979).
[24] J. Raynal, computer code ECIS95, NEA0850-14.
[25] M. C. Mermaz *et al.*, Z. Phys. A **326**, 353 (1987).
[26] J. Barrette *et al.*, Phys. Lett. **B209**, 182 (1988).